Singlet Oxygen Generation by UVA Light Exposure of Endogenous Photosensitizers

Jürgen Baier,* Tim Maisch,* Max Maier,† Eva Engel,‡ Michael Landthaler,* and Wolfgang Bäumler*
*Department of Dermatology, †Department of Physics, and ‡Department of Organic Chemistry, University of Regensburg, Regensburg, Germany

ABSTRACT UVA light (320–400 nm) has been shown to produce deleterious biological effects in tissue due to the generation of singlet oxygen by substances like flavins or urocanic acid. Riboflavin, flavin mononucleotide (FMN), flavin adenine dinucleotide (FAD), β-nicotinamide adenine dinucleotide (NAD), and β-nicotinamide adenine dinucleotide phosphate (NADP), urocanic acid, or cholesterol in solution were excited at 355 nm. Singlet oxygen was directly detected by time-resolved measurement of its luminescence at 1270 nm. NAD, NADP, and cholesterol showed no luminescence signal possibly due to the very low absorption coefficient at 355 nm. Singlet oxygen luminescence of urocanic acid was clearly detected but the signal was too weak to quantify a quantum yield. The quantum yield of singlet oxygen was precisely determined for riboflavin ($\Phi_\Delta = 0.54 \pm 0.07$), FMN ($\Phi_\Delta = 0.51 \pm 0.07$), and FAD ($\Phi_\Delta = 0.07 \pm 0.02$). In aerated solution, riboflavin and FMN generate more singlet oxygen than exogenous photosensitizers such as Photofrin, which are applied in photodynamic therapy to kill cancer cells. With decreasing oxygen concentration, the quantum yield of singlet oxygen generation decreased, which must be considered when assessing the role of singlet oxygen at low oxygen concentrations (inside tissue).

INTRODUCTION

The UVA component of solar radiation (320–400 nm) has been shown to produce deleterious biological effects in which singlet oxygen ($^1\Delta_g$ of O_2) plays a major role (1). This must have an effect on all tissue that gets into contact with UVA light, particularly the skin and the eye.

Skin is the largest body organ and is frequently exposed to sunlight, and UVA exposure is thought to cause skin aging and skin cancer mainly by singlet oxygen (2,3). Singlet oxygen mediates gene regulation via the transcription factor AP-2 (4). It activates stress-activated protein kinases (5), or it induces in skin fibroblasts a pattern of mitogen-activated protein kinase as well as an induction of p38 and c-Jun-N-terminal kinase (6). Additionally, exposure to UVA light has been recognized as a source of aging of eye lens proteins and as a risk factor for cataract formation (7).

However, the mechanisms by which UVA light-induced photodamage occur have not been fully understood (1). UVA light is weakly absorbed by a limited number of molecules in the tissue, which may act as photosensitizers. After UVA light absorption, the photosensitizer molecules cross over to a triplet state and transfer energy to generate singlet oxygen. Some of these endogenous photosensitizers have been identified, such as flavins (8), NADH/NADPH (9), urocanic acid (1), and some sterols (10).

To provide undoubted evidence for a correlation of UVA damage in tissue and singlet oxygen, the efficacy of singlet oxygen generation (the quantum yield) must be determined for these substances. Usually, the involvement of singlet oxygen is shown indirectly by adding singlet oxygen quenchers (e.g., sodium azide, beta-carotene) (3,11,12). However, in biological systems (e.g., lipids cells) singlet oxygen is short-lived (few μs), showing a very short diffusion length (13). Thus, the quencher molecules must be present directly at the site of singlet oxygen generation with a sufficiently high concentration, which is difficult and a source of ambiguous results.

In contrast to that, singlet oxygen can be directly detected by measuring its luminescence and there is no need for any additional substances. The luminescence signal is extremely weak, but we were able to detect singlet oxygen in lipids and even in living cells (14–16). When measuring the luminescence signal, the quantum yield of singlet oxygen generation can be calculated using an exogenous photosensitizer such as perinaphthenone as reference (17,18).

Moreover, after exciting a photosensitizer, there is always a competition between the generation of oxygen radicals (type I, e.g., superoxide anion) and singlet oxygen (type II reaction). That may depend on the respective microenvironment, which can be the solvent (19), aggregation of molecules (20), or the oxygen concentration (14). It has been recently shown for exogenous photosensitizers that the quantum yield of singlet oxygen depends critically on the oxygen concentration (oxygen partial pressure, i.e., pO_2) in the respective experimental setup (14,16). This is important when comparing experiments of in vitro ($pO_2 \sim 150$ mmHg) and in vivo (e.g., skin: $pO_2 < 20$ mmHg) conditions (21). Therefore, the quantum yield of the endogenous photosensitizers should be determined not only in fully aerated solutions ($\sim$150 mmHg) but also at a very low pO_2.

The high sensitivity of our detection systems allows the measurement of the entire time course of the luminescence

Submitted January 31, 2006, and accepted for publication May 17, 2006.

Address reprint requests to Dr. Wolfgang Bäumler, Dept. of Dermatology, University of Regensburg, 93042 Regensburg, Germany. Tel.: 49-941-944-9607; Fax: 49-941-944-8943; E-mail: baeumler.wolfgang@klinik.uni-regensburg.de.

0006-3495/06/08/1452/08 $2.00

doi: 10.1529/biophysj.106.082388

signal. This yields a more precise evaluation of the generation and decay of singlet oxygen as compared to the germanium diode detectors used several years ago, particularly in the spectral range of UVA and at very low luminescence intensities. The latter is important since we reduce the oxygen concentration and we usually apply small excitation pulse energies (μJ) to avoid nonlinear behavior in the luminescence signal.

To mimic UVA light excitation of endogenous photosensitizers, the third harmonic of an Nd:YAG laser was available ($\lambda_{em} = 355$ nm). That wavelength is in the middle of the UVA light spectrum ranging from 320 to 400 nm.

MATERIALS AND METHODS

Preparation of solutions

Riboflavin (purity $\geq$ 99%), flavin mononucleotide sodium (FMN, purity $\sim$ 95%), flavin adenine dinucleotide disodium salt hydrate (FAD, purity $\geq$ 95%), β-nicotinamide adenine dinucleotide sodium salt (NAD, purity $\sim$ 95%), and β-nicotinamide adenine dinucleotide phosphate hydrate (NADP, purity $\sim$ 95%) were dissolved in H_2O (bi-distilled) at a concentration of 50 μM. Urocanic acid (purity $\geq$ 99%) and cholesterol (5-cholesten-3β-ol, purity $\geq$ 99%) were dissolved in EtOH at a concentration of 3 mM and 50 μM, respectively. All substances were purchased from Sigma-Aldrich (Steinheim, Germany). Sodium azide was purchased from Merck KGaA (Darmstadt, Germany) and the nonpolar Perinaphthenone (PN) from Acros Organics (Geel, Belgium) showing a purity of $\geq$97%. The polar Perinaphthenone (PNS) was synthesized in the Institute of Organic Chemistry, Regensburg. The synthesis of PNS was performed according to the description given by Nonell et al. (18) and high-performance liquid chromatography revealed purity of >97% (for molecular structure, see Fig. 1).

Absorption spectra

The absorption spectra of each probe were recorded at room temperature with a Beckman DU640 spectrophotometer (Beckman Instruments, Munich, Germany).

Luminescence experiments

The potential sensitizers in solutions were transferred into a cuvette (QS-1000, Hellma Optik, Jena, Germany). They were excited using a frequency-tripled Nd:YAG laser (PhotonEnergy, Ottensoos, Germany) with a repetition rate of 2.0 kHz (wavelength 355 nm, pulse duration 70 ns). The laser pulse energy for luminescence experiments was 50 μJ. The singlet oxygen luminescence at 1270 nm was detected in near-backward direction with respect to the excitation beam using an infrared sensitive photomultiplier (R5509-42, Hamamatsu Photonics Deutschland, Herrsching, Germany) with a rise-time of $\sim$3 ns. The details of the setup are described elsewhere (15). The number of laser pulses for excitation was 40,000.

Determination of singlet oxygen luminescence decay and rise-time

As shown in Baumer et al. (16), the luminescence intensity is given by

$$I(t) = \frac{C}{\tau_R^{-1} - \tau_D^{-1}}\left[\exp\left(-\frac{t}{\tau_D}\right) - \exp\left(-\frac{t}{\tau_R}\right)\right]. \quad (1)$$

The constant C was used to fit the luminescence signal. The values τ_D and τ_R are the decay and rise-times, respectively. To determine the rise and decay times of singlet oxygen, the least-square fit routine of Mathematica 4.2 (Wolfram Research, Champaign, IL) was used. The experimental error of the fit was estimated to be between 15 and 25% of the values that are determined by the fit. The low signal level in some samples requires a higher error of 25%. The decay rate of singlet oxygen K_Δ (flavins) is the reciprocal value of the rise time ($K_\Delta = 1/\tau_R$). In solution, the decay rate depends on the environment of singlet oxygen (solvent, quencher, sensitizer). Equation 2 represents the sum of different rates that represent the environment (16)

$$K_\Delta = k_\Delta + k_{\Delta S} \times [S], \quad (2)$$

where k_Δ is the singlet oxygen relaxation rate in the solution and $k_{\Delta S}$ is the rate constant per molar unit for quenching of the singlet oxygen state by the sensitizer. The value [S] is the concentration of the sensitizer. The relaxation rate of the T_1 state is the same as the rise rate of the luminescence of singlet oxygen (16). The reciprocal value of the rise rate K_{T_1} is the decay-time of the luminescence of singlet oxygen ($K_{T_1} = 1/\tau_D$). Similar to K_Δ, the rise rate K_{T_1} depends on the sum of different rates, which represent the environment

$$K_{T_1} = k_{T_1} + k_{T_1 S} \times [S] + k_{T_1 O_2} \times [O_2], \quad (3)$$

where k_{T_1} is the sensitizer relaxation rate in the solution, $k_{T_1 S}$ is the rate constant for quenching of the triplet state of the sensitizer by the sensitizer, and $k_{T_1 O_2}$ describes the quenching processes by oxygen. The values [S] and [O_2] are concentrations of sensitizer and oxygen in solution, respectively.

Determination of the singlet oxygen quantum yield

Using the Wilkinson definition (22) and the assumption of a negligible energy transfer from sensitizer S_1 state to oxygen, the singlet oxygen quantum yield Φ_Δ is given by

$$\Phi_\Delta([O_2]) = \Phi_T \times f_\Delta^T \times P_T([O_2]), \quad (4)$$

where Φ_T is the triplet quantum yield and f_Δ^T is the fraction of T_1 population of the photosensitizer quenched by an oxygen-yielding singlet oxygen. The value of f_Δ^T is ranging from 0.25 to 1 (23). The proportion of T_1 population quenched by oxygen depends on the oxygen concentration as follows:

$$P_T([O_2]) = \frac{k_{T_1 O_2} \times [O_2]}{K_{T_1}([O_2])}. \quad (5)$$

In the experiments, K_{T_1} is determined from the rise or the decay of the luminescence signals and $k_{T_1 O_2}$ is the slope of K_{T_1} values at different oxygen concentrations (see Eq. 3).

Determination of the singlet oxygen quantum yield by comparing with PNS

The singlet oxygen quantum yield Φ_Δ was determined by measuring the luminescence intensity of singlet oxygen at 1270 nm as a function of absorbed laser energy using PNS as a reference. The ratio of the singlet oxygen quantum yield Φ_Δ of two sensitizers is obtained from Eqs. 4 and 5. It is given by

$$\frac{\Phi_\Delta^{un}([O_2])}{\Phi_\Delta^{PNS}([O_2])} = \frac{\Phi_T^{un} \times f_\Delta^{T,un} \times k_{T_1 O_2}^{un} \times [O_2]}{K_{T_1}^{un}([O_2])} \times \frac{K_{T_1}^{PNS}([O_2])}{\Phi_T^{PNS} \times f_\Delta^{T,PNS} \times k_{T_1 O_2}^{PNS} \times [O_2]}, \quad (6)$$

where Φ_Δ^{PNS} is the well-known singlet oxygen quantum yield of PNS used as reference and Φ_Δ^{un} is the unknown quantum yield of the respective endogenous sensitizer. Equation 1 describes the time-dependence of the luminescence signal of singlet oxygen at 1270 nm. For $C = [T_1]_0 \times f_\Delta^T \times k_{T_1 O_2} \times [O_2]$, the integral A of Eq. 1 from $t = 0$ to ∞ gives the luminescence energy $A(O_2)$:

$$A([O_2]) = \frac{[T_1]_0 \times f_\Delta^T \times k_{T_1O_2} \times [O_2]}{K_\Delta \times K_{T_1}([O_2])}. \quad (7)$$

After light absorption of the photosensitizer, a fraction of the excited molecules in the S_1 state will populate within nanoseconds the triplet T_1-state yielding a concentration $[T_1]_0 = \Phi_T \cdot [S_1]_0$. Then, the ratio of the singlet oxygen luminescence energy of two sensitizers is given by

$$\frac{A^{un}([O_2])}{A^{PNS}([O_2])} = \frac{\Phi_T^{un} \times f_\Delta^{T,un} \times k_{T_1O_2}^{un} \times [O_2]}{K_{T_1}^{un}([O_2])} \times \frac{K_{T_1}^{PNS}([O_2])}{\Phi_T^{PNS} \times f_\Delta^{T,PNS} \times k_{T_1O_2}^{PNS} \times [O_2]} \times \frac{[S_1]_0^{un} \times K_\Delta^{PNS}}{[S_1]_0^{PNS} \times K_\Delta^{un}}. \quad (8)$$

If both sensitizers are solved in H_2O and the quenching of singlet oxygen by the sensitizer can be neglected, than $K_\Delta^{PNS} = K_\Delta^{un}$ (see Eq. 2). The concentration $[S_1]_0$ of the S_1 state depends linearly on the absorbed laser energy. The absorbed laser energy is calculated from the absorption cross-section of each sensitizer at 355 nm, which has been determined from transmission measurements of the solutions. The ratio of the slopes s of the luminescence energy of singlet oxygen versus the absorbed laser energy is as follows (see Eqs. 6 and 9):

$$\frac{s^{un}([O_2])}{s^{PNS}([O_2])} = \frac{\Phi_\Delta^{un}([O_2])}{\Phi_\Delta^{PNS}([O_2])}. \quad (9)$$

This relation is used for determination of the singlet oxygen quantum yield by comparing with PNS.

RESULTS AND DISCUSSION

Absorption cross-section of endogenous photosensitizers

The absorption cross-section spectra of the different photosensitizers are shown in Fig. 1. The present experimental setup allows the time-resolved detection of singlet oxygen luminescence at an excitation wavelength of 355 nm, which is the triplication of the frequency of an Nd:YAG laser at 1064 nm. PN and PNS (Fig. 1 *A*) exhibit high absorption values at 355 nm and are used as reference photosensitizers to calculate the singlet oxygen quantum yield of the endogenous photosensitizer. PN is a well-known, nonpolar molecule (17), which can be solved in the EtOH, whereas the polar PNS has been synthesized for the use in aqueous solvents (18). Both molecules have a high singlet oxygen quantum yield close to unity independent of the solvent.

To compare with our excitation wavelength, the absorption cross-section spectra of riboflavin, FMN, and FAD dissolved in H_2O are shown in Fig. 1 *B*. The molecules have high absorption values for wavelengths shorter than 300 nm, but also from 350 to 550 nm. The light of our excitation laser (355 nm) is well absorbed in these molecules.

The absorption cross-section of NAD, NADP (dissolved in H_2O), urocanic acid, and cholesterol (dissolved in EtOH) at 355 nm are shown in Table 1. Although the absorption cross sections are very low at 355 nm, we included these compounds in our luminescence measurements due to the high sensitivity of our experimental setup. However, no luminescence at 1270 nm could be detected for NAD, NADP, and cholesterol, which is very likely due to the very low absorption cross sections at the excitation wavelength, in particular for sterols (10).

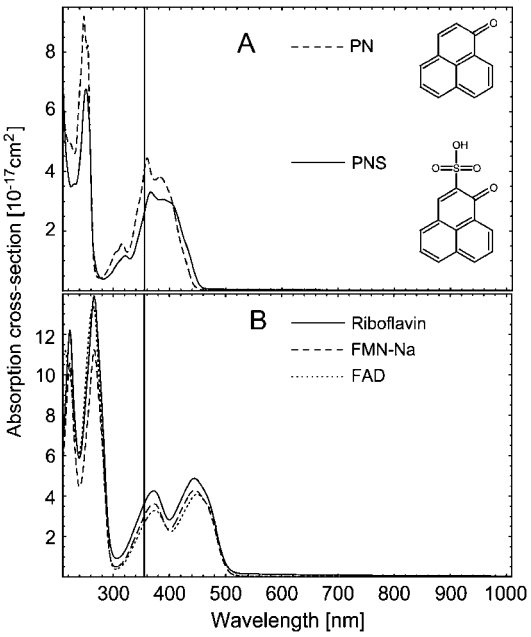

FIGURE 1 Absorption cross-section spectra of cell components: (*A*) PN in H_2O and PNS in EtOH. (*B*) Riboflavin, FMN, and FAD in H_2O. The vertical line is at 355 nm.

Singlet oxygen luminescence of urocanic acid and flavins

There was singlet oxygen luminescence upon exciting 3 mM urocanic acid. The luminescence decay time in air-saturated solution (EtOH) was 13 ± 3 μs, which is the typical decay time of singlet oxygen in ethanol (22). By adding 500 μM sodium azide to urocanic acid solution, the luminescence signal completely disappeared. Thus, the luminescence photons at 1270 nm are a direct proof of singlet oxygen, which has been generated by irradiation of urocanic acid with UVA light at 355 nm. Our result confirms the published results when using the photoacoustic detection of singlet oxygen (1). Due to the weak luminescence signal, the quantum yield of singlet oxygen could be not determined for urocanic acid.

When exciting flavin molecules, a clear luminescence signal was detected in air-saturated water. Fig. 2 *B* shows exemplarily the luminescence at 1270 nm of riboflavin (50 μM). By adding the singlet oxygen quencher sodium azide (500 μM), the decay time was significantly shortened (Fig. 2 *C*). To compare with flavins, the singlet oxygen luminescence of 50 μM PNS (Fig. 2 *A*) was detected. The solid lines in Fig. 2 are the respective fits. The singlet oxygen luminescence of excited PNS rises with 2.3 ± 0.5 μs and

TABLE 1 Spectroscopic data of photosensitizers

Photosensitizer	σ_{abs} (355 nm) (10^{-17}cm^2)	$(k_\Delta)^{-1}$ (μs)	Φ_T	Φ_Δ	
PN	4.06	14 ± 2*	1.00 (17)	0.98 ± 0.08	(17)
				0.93 ± 0.08	(18)
PNS	2.62	3.4 ± 0.5†	1.00 (17)	0.98 ± 0.08	(17)
				0.97 ± 0.06	(18)
Riboflavin	3.64	3.2 ± 0.5†	0.61 (28)	Using Φ_T, P_T, f_Δ^T:	
			0.38 (29)	0.59 ± 0.07‡	This work ($pO_2 \sim 150$ mmHg)
				0.09 ± 0.03§	
				Using PNS 0.54 ± 0.07	
FMN	3.01	3.7 ± 0.5†	—	Using PNS 0.51 ± 0.07	This work ($pO_2 \sim 150$ mmHg)
FAD	2.66	3.5 ± 0.5†	—	Using PNS 0.07 ± 0.02	This work ($pO_2 \sim 150$ mmHg)
Urocanic acid	0.17	13 ± 3*	—	¶	
NAD	0.04	**	—	—	
NADP	0.02	**	—	—	
Cholesterol	0.05	**	—	—	

*Dissolved in EtOH.
†Dissolved in H_2O.
‡$\Phi_{\Delta,max}$ calculated using Eq. 4, $f_\Delta^T = 1$ and Φ_T given Chacon et al. (28).
§$\Phi_{\Delta,min}$ calculated using Eq. 4, $f_\Delta^T = 0.25$ and Φ_T given by Islam et al. (29).
¶Signal/noise ratio was too low to determine Φ_Δ.
**No signal was detected.

decays with 3.4 ± 0.5 μs. For riboflavin in air-saturated solution, the signal rises with a time constant of 3.3 ± 0.5 μs and decays with a time constant of 3.2 ± 0.5 μs. The respective rise times represent the values of singlet oxygen in pure water (14,15). By adding 500 μM sodium azide to the 50 μM riboflavin solution, both the luminescence intensity and the decay time of singlet oxygen decreased, yielding a decay time of 1.8 ± 0.5 μs, which confirms the singlet oxygen luminescence.

Quantum yield of singlet oxygen Φ_Δ

Comparable to exogenous photosensitizers, endogenous molecules absorb UVA light in the skin and can generate singlet oxygen. The efficacy of a molecule to generate singlet oxygen is expressed by the quantum yield of singlet oxygen (Φ_Δ). The molecules such as the flavins or urocanic acid are assumed to play a major role regarding the photooxidative damage of the skin (1,3,4,6,7,24,25) and the eye lens (8,26). Thus, the quantum yield must be determined as precisely as possible. When looking at the pathways within the photosensitizer after UVA-light absorption, the quantum yield Φ_Δ depends on the triplet yield Φ_T, the triplet decay rate K_{T_1}, the rate constant $k_{T_1O_2}$, and the fraction f_Δ^T (see Eqs. 4 and 5). That approach is frequently used to calculate the quantum yield Φ_Δ (27). Thus, these rates and rate constants must be determined, which was performed for the flavin molecules riboflavin, FMN, and FAD.

Determination of Φ_Δ of riboflavin at different oxygen concentrations

Additionally, we were interested in the quantum yield at different oxygen concentrations. Therefore, the rates were determined in a range of $[O_2] = 10$–280 μM corresponding to a range of oxygen partial pressure of ~5–150 Torr (mmHg). That covers the conditions of singlet oxygen generation in vitro (~150 mmHg) and in vivo (10–20 mmHg).

Starting with riboflavin, the rates K_{T_1} and $k_{T_1O_2}$ were determined. Firstly, the singlet oxygen luminescence was measured at different photosensitizer concentrations (0.01 mM to 0.1 mM) at $[O_2] = 170 \pm 10$ μM. In Fig. 3 *A*, the Stern-Volmer shows a constant singlet oxygen relaxation rate K_Δ within the experimental accuracy. According to Eq. 2, this yields the quenching rate constant of singlet oxygen by riboflavin ($k_{\Delta S} = 0$). Extrapolation to zero riboflavin concentration yields the lifetime of singlet oxygen in pure water as $\tau_\Delta = 1/k_\Delta = 3.2 \pm 0.5$ μs, which is in excellent correlation with other experiments (15). According to Fig. 3 *A*, the relaxation rate of the triplet T_1 state of riboflavin is also constant ($k_{T_1S} = 0$) within experimental accuracy, exhibiting a value of $K_{T_1} = 0.19 \pm 0.05$ μs^{-1}.

After that, the singlet oxygen luminescence was measured at different oxygen concentrations using a constant riboflavin concentration of 50 μM. In Fig. 3 *B*, the Stern-Vollmer plot shows the dependence of the relaxation rates of the riboflavin triplet T_1 state K_{T_1} and of singlet oxygen K_Δ on the oxygen concentration in solution for riboflavin. The relaxation rate K_{T_1} shows a linear dependence on the oxygen concentration ($[O_2] = 10$ μM–280 μM). According to Eq. 3, the slope of the linear fit of the data yields the rate constant for the deactivation of riboflavin triplet T_1 state by oxygen with $k_{T_1O_2} = 1.0 \pm 0.2$ μs^{-1} mM^{-1}. Extrapolation of the linear fit to $[O_2] = 0$ (assuming $k_{T_1S} = 0$) yields the relaxation rate of riboflavin triplet T_1 state in pure water $k_{T_1} = 0.0083 \pm 0.0016$ μs^{-1}. Thus, the lifetime of the triplet T_1 state of riboflavin in pure water is $\tau_{T_1} = 120 \pm 24$ μs. This value is larger than reported previously ($\tau = 42$ μs) (8). According to

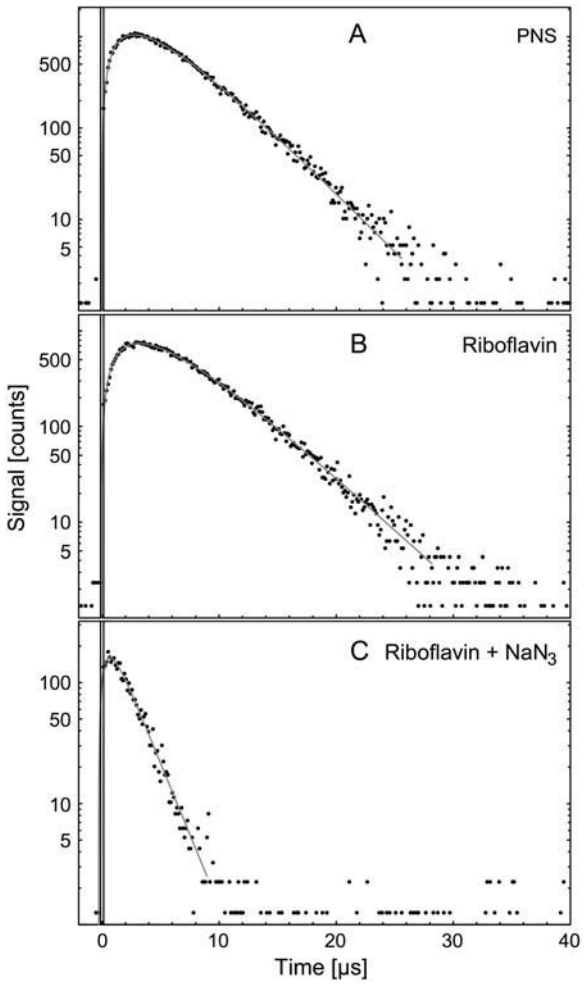

FIGURE 2 Luminescence of singlet oxygen at 1270 nm generated by aqueous solution of (*A*) 50 μM PNS, (*B*) 50 μM riboflavin, and (*C*) 50 μM riboflavin with 50 mM NaN_3 versus time. The solid curves have been fitted to the experimental data points using Eq. 1.

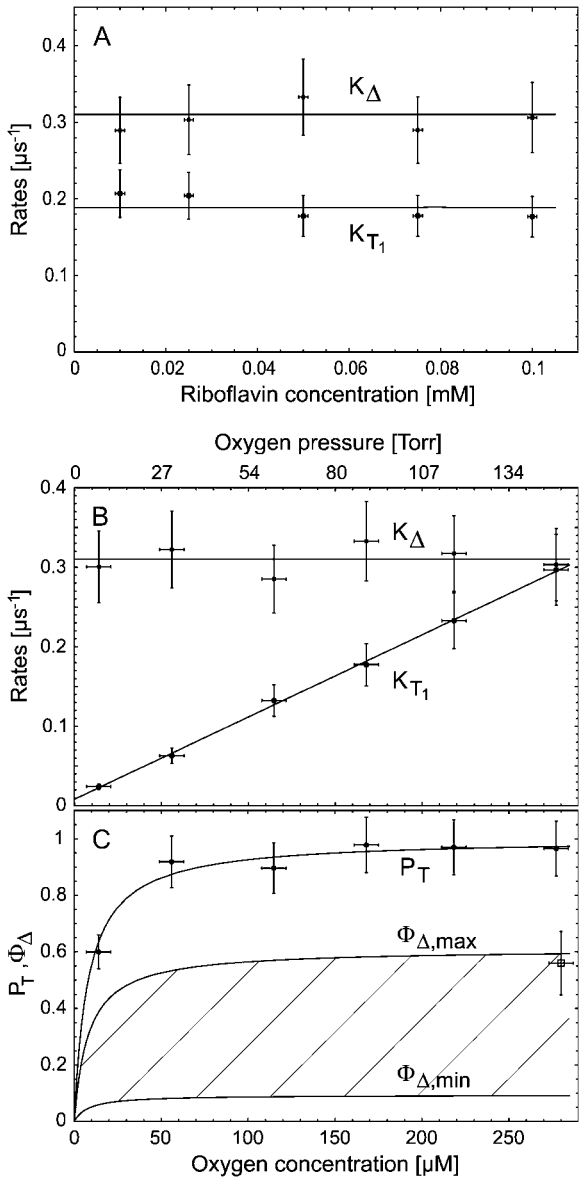

FIGURE 3 Dependence of the relaxation rates K_Δ of singlet oxygen and K_{T_1} of triplet state of riboflavin on the concentration of (*A*) riboflavin in H_2O (at 170 μM oxygen concentration) and (*B*) of oxygen (at 50 μM riboflavin). The solid lines have been fitted to the experimental data points using Eqs. 2 and 3. (*C*) Dependence of the riboflavin T_1 state deactivation efficacy P_T on oxygen concentration. The solid curve has been fitted to the experimental data points using Eq. 5. The range of the singlet oxygen quantum yield Φ_Δ is shown versus oxygen concentration by using $f_\Delta^T = 0.25$ or 1 and $\Phi_T = 0.38$ or 0.61. The solid curve has been fitted by using Eq. 4.

Fig. 3 *B*, the relaxation rate of singlet oxygen $K_\Delta = k_\Delta = 0.31 \pm 0.06\ \mu s^{-1}$ ($k_{\Delta S} = 0$, Fig. 3 *A*) is independent of the oxygen concentration within the experimental accuracy.

To begin, the efficacy P_T of the T_1 state deactivation by oxygen was determined by applying Eq. 5 and the measured relaxation rates and rate constant. An aerated solution ($[O_2] \approx 280\ \mu M$) yields $P_T = 0.97 \pm 0.10$. With decreasing oxygen concentrations, P_T is decreasing in particular, for $[O_2] < 50\ \mu M$. Since for $[O_2] = 0$ the value for P_T should theoretically be zero, the values in Fig. 3 *C* are fitted (*solid line*) accordingly using Eq. 5, including the rates which were appointed before.

Using the values of P_T, the quantum yield of singlet oxygen can be calculated by using $\Phi_\Delta([O_2]) = \Phi_T \cdot f_\Delta^T \cdot P_T([O_2])$ (Eq. 4). However, for Φ_T, only two values are available, being quite different with $\Phi_T = 0.61$ (28) and $\Phi_T = 0.38 \pm 0.05$ (29). Additionally, no values are available for f_Δ^T, which can range between 0.25 and 1, depending on the triplet state energy E_{T_1} and the polarity of the solvent (23).

Thus, Φ_Δ of riboflavin can be calculated only within a range that is shown as a hatched area in Fig. 3 *C*, whereas the line $\Phi_{\Delta,max}(\Phi_T = 0.61, f_\Delta^T = 1)$ and $\Phi_{\Delta,min}$ ($f_\Delta^T = 0.25$, $\Phi_T = 0.38$) is calculated. Thus, in aerated solution ($[O_2] = 280\ \mu M$), the highest value is $\Phi_{\Delta,max} = 0.59 \pm 0.07$ and the minimal value is $\Phi_{\Delta,min} = 0.09 \pm 0.03$.

This experimental approach shows the clear dependence of the quantum yield on the oxygen concentration. The value

Φ_Δ decreases with decreasing oxygen concentrations, which is very impressive for the line $\Phi_{\Delta,max}$. When looking at the line $\Phi_{\Delta,min}$, the values are not so different in the entire range of oxygen concentration. It is therefore important to know the true value of Φ_Δ, which might be in the range of 0.09 to 0.59 under the in vitro conditions ($[O_2] = 280\ \mu M$). This is disappointing but comparable to problems with exogenous photosensitizers. For example, when investigating the photosensitizer Photofrin I in water, Φ_Δ values were determined with 0.06 (H_2O), high oxygen concentration (30); 0.12 (D_2O) aerated (31); 0.35 (D_2O), high oxygen concentration (32); or even 0.77 (D_2O) aerated (33).

To assess the role of endogenous sensitizers regarding UVA light, especially when looking at the biological effects attributed to singlet oxygen, precise values are necessary. Since there are hardly any values available for Φ_T or f_Δ^T, the determination of Φ_Δ of riboflavin and the other flavins was performed by using another approach.

Determination of Φ_Δ of all flavins by comparing with PNS

Since the range of possible values of Φ_Δ is maximal at high oxygen concentrations, the following experiments were carried out at $[O_2] = 280\ \mu M$. The values Φ_Δ of flavins (riboflavin, FMN, and FAD) were determined by comparing quantitatively the luminescence signal at 1270 nm to luminescence signal of PNS. Both Perinaphthenones are well-characterized molecules exhibiting a Φ_Δ of close to unity (see Table 1). Fig. 4 shows the dependence of time-integrated signal of luminescence of singlet oxygen at 1270 nm on absorbed laser energy for PNS and for the endogenous photosensitizers riboflavin, FMN, and FAD at equal concentrations of 50 μM. The time-integrated signal increased linearly with increasing absorbed excitation energy, whereas the respective fits are shown as solid lines.

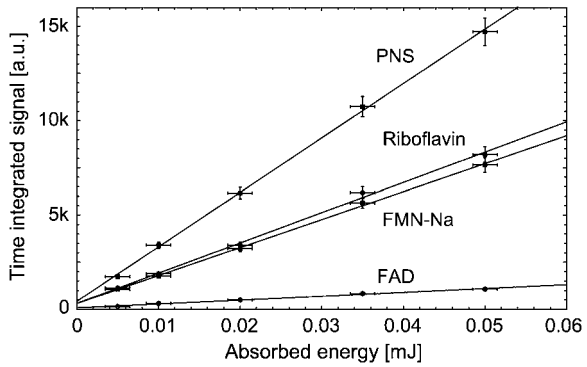

FIGURE 4 Time-integrated signal of luminescence of singlet oxygen at 1270 nm versus absorbed energy for air-saturated solutions of PNS, riboflavin, FMN, and FAD in H_2O. Each slope is corrected by the absorption of the sensitizers at 355 nm. The solid lines have been fitted to the experimental data points using a simple linear fit ($y(x) = ax + b$).

The ratio of the slopes is the same as the ratio of the singlet oxygen quantum yields with PNS as reference, respectively (Eq. 8). The absorbed energy has been calculated from the incident laser energy by using the different absorption cross sections of each sensitizer at 355 nm. In Table 1 the singlet oxygen quantum yields are shown for PNS and PN as reference and the calculated values of riboflavin ($\Phi_\Delta = 0.54 \pm 0.07$), FMN ($\Phi_\Delta = 0.51 \pm 0.07$), and FAD ($\Phi_\Delta = 0.07 \pm 0.02$). The Φ_Δ value of riboflavin in aerated solution is added to Fig. 3 *C*, which is in good correlation to $\Phi_{\Delta,max}$ of 0.59 within the experimental accuracy and the value determined by Chacon et al. (28). This may lead to the suggestion that the value of Φ_T is $\sim$0.6 and $f_\Delta^T \approx 1$. Consequently, for molecules such as riboflavin, the line $\Phi_{\Delta,max}$ is valid (Fig. 3 *C*) regarding the dependence of quantum yield on the oxygen concentration.

Riboflavin and FMN exhibit quantum yields higher than for exogenous photosensitizers such as hematoporphyrin derivative (Photofrin, $\Phi_\Delta = 0.35$) (20), which are used in photodynamic therapy to kill cancer cells. Our results confirm that riboflavin and FMN are potential type II sensitizers under fully aerated conditions. Even the complex molecule FAD retains the ability of the flavin group to generate singlet oxygen. Interestingly, the quantum yield decreases with complexity of molecules going from riboflavin, to FMN and to FAD.

The role of oxygen concentration

The detection of singlet oxygen by its luminescence is a powerful tool even in living cells in vitro (15,34). As already stated above, the efficacy of singlet oxygen generation decreases with decreasing oxygen concentration, i.e., decreasing oxygen partial pressure. That is shown in Fig. 3 *C* ($\Phi_{\Delta,max}$) for riboflavin, which is similar to other sensitizers (14,16) and the other flavins. To elucidate the role of flavins, experiments are carried out frequently in vitro under aerated conditions, which is equivalent to an oxygen partial pressure of $\sim$150 Torr (150 mmHg or $[O_2] = 280\ \mu M$). Under in vivo conditions, e.g., in living skin, the oxygen partial pressure is only 20 Torr (20 mmHg or $[O_2] = 37\ \mu M$) at the dermal-epidermal junction or even less inside the cells (21). In view of this difference in oxygen partial pressure, the singlet oxygen generation by riboflavin decreases approximately twofold at most. These results are important when comparing experiments that are performed at different oxygen partial pressure.

Recently, it was shown that irradiated riboflavin can damage nicotine by antibody-catalyzed oxidative degradation (35). However, that experiment was performed in aerated solution and therefore at a high efficacy of singlet oxygen generation, which might not reflect the degradation under low oxygen conditions in vivo. Riboflavin-sensitized photodynamic modifications of high-molecular-weight Kininogen were also investigated only in vitro and singlet oxygen was found to be an important mediator (36). According to experiments under aerobic conditions it was stated that

photoexcitation of riboflavin may also potentially occur in vivo in the organs and tissues that are permeable to light, such as the eye or skin, and damage hyaluronic acid and other cell-matrix components, to cause inflammation and accelerate aging (37). In view of our results, one must be careful when judging the relevance of singlet oxygen in vivo based on experiments in vitro.

Additionally, after excitation of sensitizers such as riboflavin, there is always a competition between the generation of oxygen radicals (type I) and singlet oxygen (type II reaction). That competition depends on the oxygen concentration in the respective experimental setup. At fully aerated conditions ($[O_2] \approx 280\ \mu M$), the UVA light is effectively converted to singlet oxygen ($\Phi_\Delta = 0.54$). At low oxygen concentrations ($[O_2] < 2\ \mu M$), the singlet generation decreases to $\Phi_\Delta < 0.20$. This is important since most of the endogenous photosensitizers are located inside cells and the oxygen partial pressure inside a cell can be 4 Torr ($[O_2] = 7.5\ \mu M$) and even less (38). At the same time, the generation of other reactive oxygen species (e.g., oxygen radicals) may increase. This correlates well to findings that riboflavin solution showed stronger cytotoxicity during irradiation under hypoxia than under air due to the heightened generation of H_2O_2 (39). Our results also support the very recent findings that the inactivation of 6-phosphate dehydrogenase (G6PD) results from its direct oxidation by the excited triplet state of riboflavin in a Type-I-photosensitized reaction whose efficiency increases at low oxygen concentration (40).

CONCLUSIONS

In the last decade, numerous articles have stated that UVA light exposure cause skin aging or even skin cancer mainly by singlet oxygen (1,3–7,24,41,42). However, precise measurements of singlet oxygen generation by endogenous photosensitizers were missing, in particular at different oxygen concentrations.

Applying UVA light to urocanic acid, singlet oxygen luminescence was clearly detected, but the signal was too weak to quantify the respective quantum yield. Exciting riboflavin, FMN, and FAD, strong luminescence signal of singlet oxygen was detected. For these substances the quantum yield were successfully determined in air-saturated solvents using PNS as reference (riboflavin $\Phi_\Delta = 0.54 \pm 0.07$, FMN $\Phi_\Delta = 0.51 \pm 0.07$, and FAD $\Phi_\Delta = 0.07 \pm 0.02$). Depending on their concentration in the skin, the flavins are potential generators of singlet oxygen, even more effective than exogenous porphyrins used for cell killing in photodynamic therapy. In view of these high values, it seems to be reasonable that these substances including urocanic acid can provide sufficient singlet oxygen during UVA exposure leading to gene regulation, photoaging, and even carcinogenesis.

When measuring the efficacy of singlet oxygen generation at different oxygen concentrations, the efficacy of singlet oxygen generation (P_T) decreased significantly for low oxygen concentrations. When irradiating, e.g., riboflavin with UVA light, at least a factor-2-less singlet oxygen is generated in the skin as compared to the condition in an aerated environment (e.g., in vitro).

This work was supported by the Dr. Heinz Maurer Foundation, Germany.

REFERENCES

1. Hanson, K. M., and J. D. Simon. 1998. Epidermal trans-urocanic acid and the UV-A-induced photoaging of the skin. *Proc. Natl. Acad. Sci. USA.* 95:10576–10578.
2. Berneburg, M., H. Plettenberg, K. Medve-Konig, A. Pfahlberg, H. Gers-Barlag, O. Gefeller, and J. Krutmann. 2004. Induction of the photoaging-associated mitochondrial common deletion in vivo in normal human skin. *J. Invest. Dermatol.* 122:1277–1283.
3. Wertz, K., P. Hunziker, N. Seifert, G. Riss, M. Neeb, G. Steiner, W. Hunziker, and R. Goralczyk. 2005. Beta-carotene interferes with ultraviolet light A-induced gene expression by multiple pathways. *J. Invest. Dermatol.* 124:428–434.
4. Grether-Beck, S., S. Olaizola-Horn, H. Schmitt, M. Grewe, A. Jahnke, J. P. Johnson, K. Briviba, H. Sies, and J. Krutmann. 1996. Activation of transcription factor AP-2 mediates UVA radiation- and singlet oxygen-induced expression of the human intercellular adhesion molecule 1 gene. *Proc. Natl. Acad. Sci. USA.* 93:14586–14591.
5. Kick, G., G. Messer, G. Plewig, P. Kind, and A. E. Goetz. 1996. Strong and prolonged induction of c-Jun and c-Fos proto-oncogenes by photodynamic therapy. *Br. J. Cancer.* 74:30–36.
6. Klotz, L. O., C. Pellieux, K. Briviba, C. Pierlot, J. M. Aubry, and H. Sies. 1999. Mitogen-activated protein kinase (p38-, JNK-, ERK-) activation pattern induced by extracellular and intracellular singlet oxygen and UVA. *Eur. J. Biochem.* 260:917–922.
7. McCarty, C. A., and H. R. Taylor. 1996. Recent developments in vision research: light damage in cataract. *Invest. Ophthalmol. Vis. Sci.* 37:1720–1723.
8. Viteri, G., A. M. Edwards, J. De la Fuente, and E. Silva. 2003. Study of the interaction between triplet riboflavin and the α-, βH- and βL-crystallins of the eye lens. *Photochem. Photobiol.* 77:535–540.
9. Sohal, R. S., and R. Weindruch. 1996. Oxidative stress, caloric restriction, and aging. *Science.* 273:59–63.
10. Albro, P. W., P. Bilski, J. T. Corbett, J. L. Schroeder, and C. F. Chignell. 1997. Photochemical reactions and phototoxicity of sterols: novel self-perpetuating mechanisms for lipid photooxidation. *Photochem. Photobiol.* 66:316–325.
11. Trekli, M. C., G. Riss, R. Goralczyk, and R. M. Tyrrell. 2003. Beta-carotene suppresses UVA-induced HO-1 gene expression in cultured FEK4. *Free Radic. Biol. Med.* 34:456–464.
12. Le Panse, R., L. Dubertret, and B. Coulomb. 2003. p38 Mitogen-activated protein kinase activation by ultraviolet A radiation in human dermal fibroblasts. *Photochem. Photobiol.* 78:168–174.
13. Bronshtein, I., M. Afri, H. Weitman, A. A. Frimer, K. M. Smith, and B. Ehrenberg. 2004. Porphyrin depth in lipid bilayers as determined by iodide and parallax fluorescence quenching methods and its effect on photosensitizing efficiency. *Biophys. J.* 87:1155–1164.
14. Engl, R., R. Kilger, M. Maier, K. Scherer, C. Abels, and W. Baumler. 2002. Singlet oxygen generation by 8-methoxypsoralen in deuterium oxide: relaxation rate constants and dependence of the generation efficacy on the oxygen partial pressure. *J. Phys. Chem. B.* 106:5776–5781.
15. Baier, J., M. Maier, R. Engl, M. Landthaler, and W. Baumler. 2004. Time-resolved investigations of singlet oxygen luminescence in water, in phosphatidylcholine, and in aqueous suspensions of phosphatidylcholine or HT29-cells. *J. Phys. Chem. B.* 109:3041–3046.

16. Baumer, D., M. Maier, R. Engl, R. M. Szeimies, and W. Baumler. 2002. Singlet oxygen generation by 9-acetoxy-2,7,12,17-tetrakis-(β-methoxyethyl)-porphycene (ATMPn) in solution. *Chem. Phys.* 285: 309–318.

17. Schmidt, R., C. Tanielian, R. Dunsbach, and C. Wolff. 1994. Perinaphthenone, a universal reference compound for the determination of quantum yields of singlet oxygen $O_2(^1\Delta_g)$ sensitization *J. Photochem. Photobiol. A.* 79:11–17.

18. Nonell, S., M. Gonzalez, and F. M. Trull. 1993. ^{1}H-Phenalen-1-one-sulfonic acid: an extremely efficient singlet molecular oxygen sensitizer for aqueous media. *Afinidad.* 448:445–450.

19. Vakrat-Haglili, Y., L. Weiner, V. Brumfeld, A. Brandis, Y. Salomon, B. McLlroy, B. C. Wilson, A. Pawlak, M. Rozanowska, T. Sarna, and A. Scherz. 2005. The microenvironment effect on the generation of reactive oxygen species by Pd-bacteriopheophorbide. *J. Am. Chem. Soc.* 127:6487–6497.

20. Tanielian, C., C. Schweitzer, R. Mechin, and C. Wolff. 2001. Quantum yield of singlet oxygen production by monomeric and aggregated forms of hematoporphyrin derivative. *Free Radic. Biol. Med.* 30:208–212.

21. Baumgärtl, H., A. Ehrly, K. Saeger-Lorenz, and D. Lübbers. 1987. Clinical Oxygen Pressure Measurement. A. M. Ehrly, J. Hauss, and R. Huch, editors. Springer, Berlin, Germany.

22. Wilkinson, F., W. P. Helman, and A. B. Ross. 1995. Rate constants for the decay and reactions of the lowest electronically excited singlet state of molecular oxygen in solution. An expanded and revised compilation. *J. Phys. Chem. Ref. Data.* 24:663–1021.

23. Schmidt, R., and F. J. Shafii. 2001. The influence of charge transfer interactions on the sensitization of singlet oxygen: formation of $O_2(1\sigma_g^+)$, $O_2(^1\Delta_g)$ and $O_2(3\sigma_g^-)$ during oxygen quenching of triplet excited biphenyl derivatives. *J. Phys. Chem. A.* 105:8871–8877.

24. Berneburg, M., T. Gremmel, V. Kurten, P. Schroeder, I. Hertel, A. von Mikecz, S. Wild, M. Chen, L. Declercq, M. Matsui, T. Ruzicka, and J. Krutmann. 2005. Creatine supplementation normalizes mutagenesis of mitochondrial DNA as well as functional consequences. *J. Invest. Dermatol.* 125:213–220.

25. Martinez, G. R., A. P. Loureiro, S. A. Marques, S. Miyamoto, L. F. Yamaguchi, J. Onuki, E. A. Almeida, C. C. Garcia, L. F. Barbosa, M. H. Medeiros, and P. Di Mascio. 2003. Oxidative and alkylating damage in DNA. *Mutat. Res.* 544:115–127.

26. Ortwerth, B. J., V. Chemoganskiy, and P. R. Olesen. 2002. Studies on singlet oxygen formation and UVA light-mediated photobleaching of the yellow chromophores in human lenses. *Exp. Eye Res.* 74:217–229.

27. Gorman, A., and M. A. Rodgers. 1992. Current perspectives of singlet oxygen detection in biological environments. *J. Photochem. Photobiol. B.* 14:159–176.

28. Chacon, J. N., J. McLearie, and R. S. Sinclair. 1988. Singlet oxygen yields and radical contributions in the dye-sensitised photo-oxidation in methanol of esters of polyunsaturated fatty acids (oleic, linoleic, linolenic and arachidonic). *Photochem. Photobiol.* 47:647–656.

29. Islam, S., A. Penzkofer, and P. Hegemann. 2003. Quantum yield of triplet formation of riboflavin in aqueous solution and of flavin mononucleotide bound to the LOV1 domain of Phot1 from *Chlamydomonas reinhardtii*. *Chem. Phys.* 291:97–114.

30. Blum, A., and L. I. Grossweiner. 1985. Singlet oxygen generation by hematoporphyrin IX, uroporphyrin I and hematoporphyrin derivative at 546 nm in phosphate buffer and in the presence of egg phosphatidylcholine liposomes. *Photochem. Photobiol.* 41:27–32.

31. Murasecco, P., E. Oliveros, A. M. Braun, and P. Monnier. 1985. Quantum yield measurements of the haematoporphyrin derivate (HPD) sensitized singlet oxygen production. *Photobiochem. Photobiophys.* 9: 193–201.

32. Kessel, D., T. J. Dougherty, and T. G. Truscott. 1988. Photosensitization by diporphyrins joined via methylene bridges. *Photochem. Photobiol.* 48:741–744.

33. Egorov, S. Y., A. Y. Tauber, A. A. Krasnovsky, A. N. Nizhnik, A. Y. Nockel, and A. F. Mironov. 1989. Photogeneration of singlet molecular oxygen by the components of hematoporphyrin IX derivative. *Byull. Eksp. Biol. Med.* 10:440–442.

34. Snyder, J. W., E. Skovsen, J. D. Lambert, and P. R. Ogilby. 2005. Subcellular, time-resolved studies of singlet oxygen in single cells. *J. Am. Chem. Soc.* 127:14558–14559.

35. Dickerson, T. J., N. Yamamoto, and K. D. Janda. 2004. Antibody-catalyzed oxidative degradation of nicotine using riboflavin. *Bioorg. Med. Chem.* 12:4981–4987.

36. Baba, S. P., D. K. Patel, and B. Bano. 2004. Modification of sheep plasma kininogen by free radicals. *Free Radic. Res.* 38:393–403.

37. Frati, E., A. M. Khatib, P. Front, A. Panasyuk, F. Aprile, and D. R. Mitrovic. 1997. Degradation of hyaluronic acid by photosensitized riboflavin in vitro. Modulation of the effect by transition metals, radical quenchers, and metal chelators. *Free Radic. Biol. Med.* 22:1139–1144.

38. Schenkman, K. A. 2001. Cardiac performance as a function of intracellular oxygen tension in buffer-perfused hearts. *Am. J. Physiol. Heart Circ. Physiol.* 281:2463–2472.

39. Minami, H., K. Sato, T. Maeda, H. Taguchi, K. Yoshikawa, H. Kosaka, T. Shiga, and T. Tsuji. 1999. Hypoxia potentiates ultraviolet A-induced riboflavin cytotoxicity. *J. Invest. Dermatol.* 113:77–81.

40. Silva, E., L. Herrera, A. M. Edwards, J. de la Fuente, and E. Lissi. 2005. Enhancement of riboflavin-mediated photo-oxidation of glucose 6-phosphate dehydrogenase by urocanic acid. *Photochem. Photobiol.* 81:206–211.

41. Berneburg, M., S. Grether-Beck, V. Kurten, T. Ruzicka, K. Briviba, H. Sies, and J. Krutmann. 1999. Singlet oxygen mediates the UVA-induced generation of the photoaging-associated mitochondrial common deletion. *J. Biol. Chem.* 274:15345–15349.

42. Schieke, S. M., C. von Montfort, D. P. Buchczyk, A. Timmer, S. Grether-Beck, J. Krutmann, N. J. Holbrook, and L. O. Klotz. 2004. Singlet oxygen-induced attenuation of growth factor signaling: possible role of ceramides. *Free Radic. Res.* 38:729–737.